Deriving Useful Information from Bimonthly Global-Scale Climate Analysis for Climate Change Adaptation Over East Africa

Isaac K. Tetteh, Nana K.A. Appiah-Badu, Fredrick H.M. Semazzi and Olawale E. Olayide

1   Introduction

Effective planning and execution of climate change adaptations is expected to bring new lease of hope to the affected societies confronted with the negative tendencies of climate change. Success of this activity to some extent is contingent on a good understanding of climate variability and change. On the global scale, eclectic adaptation strategies have evolved, or continue to evolve, in response to the specific menace created by climate variability and change, irrespective of the background driving force—natural or anthropogenic.

Interestingly, East Africa, one of the most vulnerable regions to global environmental change, has benefited from implementations of adaptation strategies derived directly or indirectly from a plethora of scholarly research efforts (e.g., Ropelewski and Halpert 1987; Ogallo 1988; Barnston and Ropelewski 1992; Funk 2012; Smith and Semazzi 2014). Such efforts have been complemented by, for example, operationalization of seasonal forecasts of long (March-April-May: MAM) and short (October-November-December: OND) rains by the Greater Horn of Africa Climate Outlook Forum (GHACOF). GHACOF is organized by the

I.K. Tetteh (✉) · O.E. Olayide
Department of Theoretical and Applied Biology, Kwame Nkrumah University
of Science and Technology (KNUST) Kumasi, Kumasi, Ghana
e-mail: iktetteh.cos@knust.edu.gh; isaac.tet@gmail.com

N.K.A. Appiah-Badu
Department of Physics, KNUST, Kumasi, Ghana

F.H.M. Semazzi
Marine, Earth, and Atmospheric Sciences, North Carolina State University,
Raleigh, NC 27695-8208, USA

O.E. Olayide
Centre for Sustainable Development, University of Ibadan, Ibadan, Nigeria

IGAD (Inter-Governmental Authority on Development) Climate Prediction and Application Centre (ICPAC), Nairobi, Kenya. It typically uses consensus forecasts, which derive inputs from empirical climate research outcomes.

Empirical climate research on rainfall variability has documented the role of interannual variability of local and remote forcings of the East African seasonal climate, which are key precursors used in operational seasonal climate prediction scheme. Interannual variability has chiefly focused on climatic and dynamic features in the annual and seasonal cycles that govern the region's long and short rainfall variability. Three important ocean-atmosphere temporal scales, which may be identified in the interannual variability and have great influence on the region's seasonal rainfall patterns, are monthly, bimonthly, and seasonal timescales (e.g. Latif et al. 1999; Saji et al. 1999; Marchant et al. 2006; Smith and Semazzi 2014). As a general summary from these collections, the region's rainfall variability points to the Pacific ENSO and Indian Ocean, and to a lesser extent the Atlantic Ocean, and their associated atmospheric dynamics. These, however, do not rule out orographic/land surface forcing and vegetation feedbacks or dynamics of the region's climate variability.

Generally, the sub-Saharan African countries are lagging far behind the advanced counterparts in efficient utilization of adaptation technologies commonly applied to ameliorate the detrimental effects of climate variability and change (Washington et al. 2006; Akponikpè et al. 2010; Ford et al. 2015). These are due to many constraints such as the lack of adaptive capacities and capital resources. Addressing these constraints is beyond the scope of the current study. However, a critical issue that warrants consideration is the need for adaptation strategy enhancement that would rely on new climate information for sustainable resilience to climate shocks. The climate information should unequivocally describe or contain features—behavior, characteristics and evolution at different timescales, as they interact with other complex climate systems or subsystems. To the best of our knowledge, among the timescales in the interannual variability, bimonthly ocean-atmosphere features have been the least studied. It is therefore justifiable to explore the potential influence of these features on the region's rainfall variability, from a global stand point. This would improve predictive understanding of the region's rains, on the premise that current numerical and statistical model predictive skills are far from perfect. Also, it would contribute to effective adaptation management, especially of sustainable agriculture, climate-induced health problems, flood and drought disasters, and other climate-sensitive socioeconomic problems.

The trust of this study was to provide useful climate information needed by end users for incorporation into sustainable climate change developmental goals. Specifically, it was designed to carry out an analysis of bimonthly evolution of global ocean-atmosphere features and their relationship to the dominant modes of MAM seasonal rainfall variability during the climatologically prominent ENSO phase. It was expected that SST sectors and their associated upper level atmospheric circulation patterns would be delineated for improving climate change adaptive capacity.

2 Data and Methods

2.1 Data

The study utilized monthly gridded precipitation, global horizontal wind and SST data. The horizontal winds at 200 hPa level were sourced from the National Centers for Environmental Prediction-National Center for Atmospheric Research (NCEP-NCAR) reanalysis (Kalnay et al. 1996). The data, covering periods from January 1948 to March 2016 on a global grid of 2.5° × 2.5° spatial resolution, are continuously updated. The precipitation dataset, with spatial resolution of 0.5° × 0.5° resolution, was sourced from Climatic Research Unit (CRU). The data was recorded from about 4000 weather stations worldwide (land only) and covered the periods from January 1901 to December 2012 (Harris et al. 2014). This dataset is periodically updated. Extended Reconstructed SST (ERSST; Smith and Reynolds 2004) data was used. The dataset extended from January 1854 to March 2016, and has a spatial resolution of 2.0° × 2.0° on a global grid. This dataset is also continuously updated.

2.2 Analysis Techniques

2.2.1 Empirical Orthogonal Function (EOF) Analysis of MAM Rainfall

Standard EOF technique (Schreck and Semazzi 2004; Wilks 2006; Hannachi et al. 2007), based on the correlation matrix, was applied to CRU MAM precipitation over East Africa covering the domain of Bowden and Semazzi (2007). The data spanned 1951–2008, which consisted of nearly 60 years of continuous data. The analysis period was based on the framework of Tetteh (2012) over West Africa, which has been extended to investigate other hypotheses over the rest of the sub-Saharan climate systems. The EOF analysis was aimed at isolating and retaining dominant, spatially coherent patterns and their associated temporal structures of the seasonal long rains. The leading modes that satisfied the sampling error criterion in the eigenvalue spectrum were retained for further analysis (North et al. 1982). In this way, EOF was viewed as exploratory data analysis tool (Johnson and Weichern 2007).

2.2.2 Construction of Standardized Global SST and Upper Level Anomalies

To investigate the influence of bimonthly global ocean SSTs and their associated atmospheric structures during the climatologically active ENSO phase, the SSTs

and horizontal winds (200 hPa) data were standardized to zero mean and unit variance, to put all the data on the same scale. This was first done by averaging the bimonthly fields before standardization for five consecutive two months period (December-January, January-February, February-March, March-April and April-May (DJ, JF, FM, MA and AM). This rolled over from 1950 to 2007 for December to 1951–2008 (from January through to May).

2.2.3 Lagged Heterogeneous Grid Point Correlations Between the Rainfall Modes and Standardized Global SSTs and Velocity Potential (Divergence) Computations

Lagged heterogeneous grid-point correlations were computed between each of the rainfall modes and the global SSTs for all the time lags until the rainfall season was over. The purpose was to evaluate, delineate and monitor the specific SST signals that were connected to the rains. A similar one was conducted for the horizontal winds (200 hPa)—zonal (u) and meridional (v), from which divergent circulation (Krishnamurti 1971) was computed, since this atmospheric flow played an important role in global monsoon dynamics (Trenberth et al. 2000).

3   Results

3.1   *East African MAM Rainfall Variability*

Figure 1 depicts the spatio-temporal patterns of the rainfall modes, in which four leading modes retained were based on the *delta-test* (North et al. 1982). These contributed to 34.2% of the total explained variance. The value signified low interannual variance of the long rains, which was consistent with previous studies (Ropelewski and Halpert 1987; Ogallo 1989). The respective contributions of precipitation EOFs 1, 2, 3, and 4 were 10.1, 9.1, 8.2, and 6.8%. Interestingly, all their EOF time series (Fig. 1e–h) demonstrated interannual variability but with differences in their amplitude of fluctuations. The precipitation patterns displayed distinct variations.

Figure 1a shows the eigenvector loadings of the precipitation EOF 1. Generally, a bipolar pattern was observed. The center of action depicted positive weights located over the greater portion of the domain, from south to northeast. The EOF 2 (Fig. 1b) also depicted a bipolar structure, but nearly antithetic to the EOF 1 pattern. Positive (negative) weights were centered over the northern (southern) sectors of the region. The EOF 3 loadings (Fig. 1c) were characterized by positive weights in the western and southern boundaries, whereas the remaining sectors contained the negative weights. The FOF 4 spatial patterns (Fig. 1d) showed small-scale positive weights confined to the horn area. Widespread negative weights were discernible in the rest of the region.
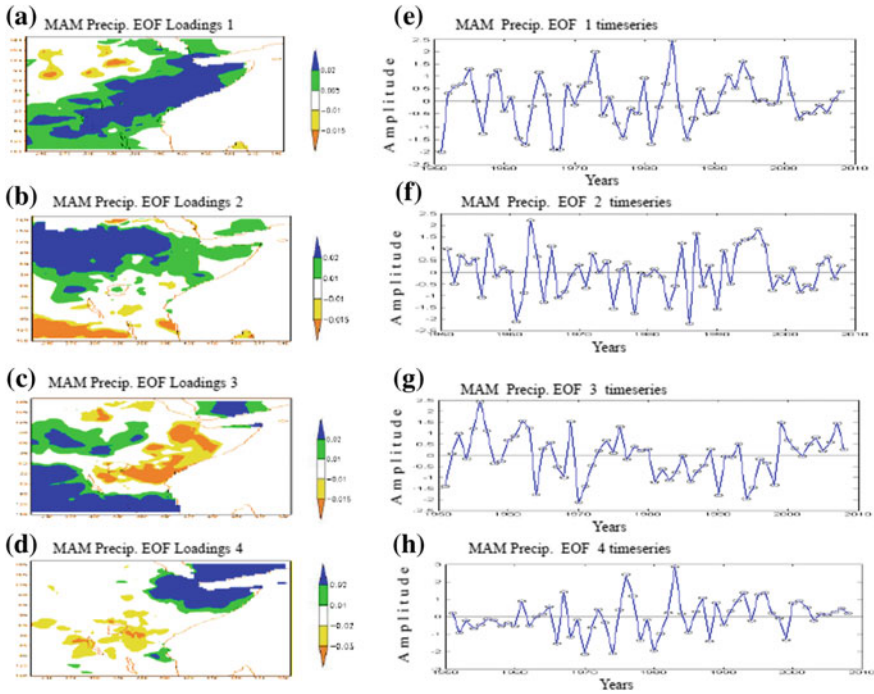
Fig. 1 Dominant modes of long rains (MAM) variability over East Africa. Panels **a–d** are the spatial patterns of the rainfall with corresponding legends. *Blue* and *green shades* depict areas of above-normal rainfall while all other shades correspond to below-normal rainfall. Panels **e–g** are the corresponding time series of the rainfall patterns

3.2   East African MAM Rainfall Modes and Global SST Relationships

In this section, grid-point correlations between the four rainfall modes and the standardized global SST anomalies are presented at various time lags (Figs. 2, 3, 4 and 5). Generally, the four modes responded differently to the Pacific ENSO, Atlantic and the Indian Oceans. Close observation showed that most of the Pacific Niños were represented. Specifically, these were Niño 3 (5° N–5° S, 150° W–90° W), Niño 3.4 (5° N–5° S, 170°–120° W) and Niño 4 (5° N–5° S, 160° E–150° W) regions. The analysis captured specific ones that had linkages to specific rainfall modes and these interactions were time-dependent.

It was noticed from Fig. 2 that the influence of global SST distributions in the tropical Pacific was strongest in DJ, but had the weakest association in AM. The DJ signal captured the climatologically active phase of ENSO, which is consistent with literature. Warm (cold) oceanic conditions in the Pacific enhanced (suppressed) convective activities associated with MAM precipitation EOF 1 mode. Other
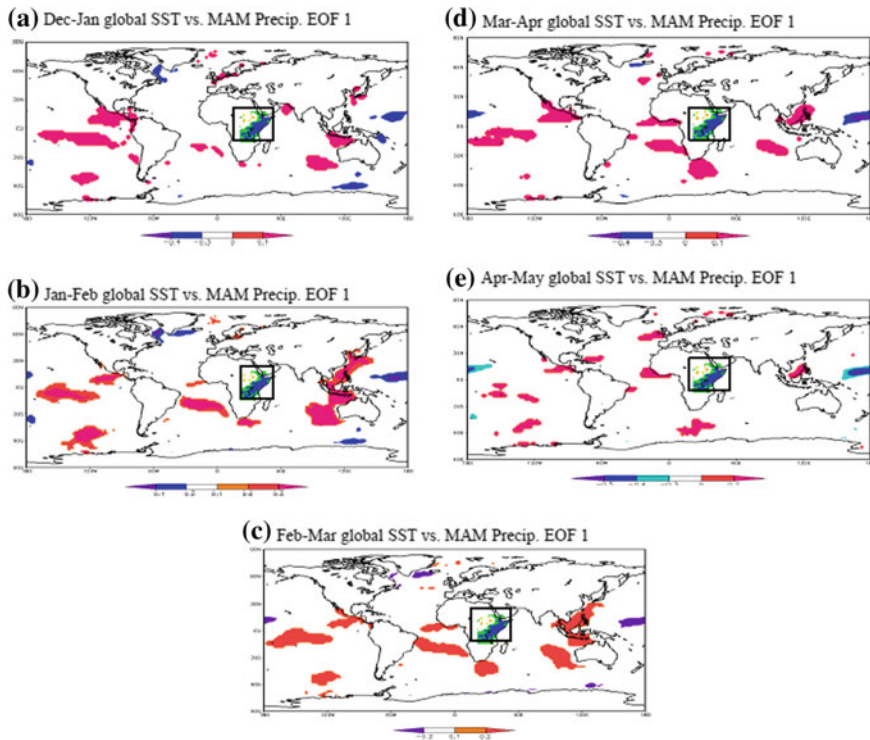
Fig. 2 Relationship between standardized bimonthly global SST anomalies and East African MAM precipitation EOF 1 time series at different time lags. Legend is for the range of correlation coefficient. Significant areas at 95% confidence level, using t-test, are *shaded*. The precipitation spatial patterns over the region are enclosed in *boxes*

features identified were the localized SST conditions in the Indian Ocean off the western seaboard of India and a more prominent one on the western-to-northern seaboard of Australia. The latter persisted up to MA, where it shifted to the vicinity of the Indian Ocean Dipole (IOD) domain (Saji et al. 1999; Marchant et al. 2006). The Indian Ocean features were in phase with the tropical Pacific conditions from DF to MA, but experienced a complete annihilation in AM. The tropical South Atlantic warming became discernible from JF up to MA and also had a good link to the precipitation mode. However, it started to weaken in AM, which indicated the onset of the cooling phase of the tropical South Atlantic Ocean—a vital driver of the West African climate.

Interestingly, precipitation EOF 2 mode in reality had no substantial relationship with the basinwide SST distributions over the study period (Fig. 3). A similar observation was made by Smith and Semazzi (2014), when they investigated the relationship between their precipitation EOF 2 mode and seasonal global SST conditions. The precipitation EOF 3 mode tended to display direct relationship with
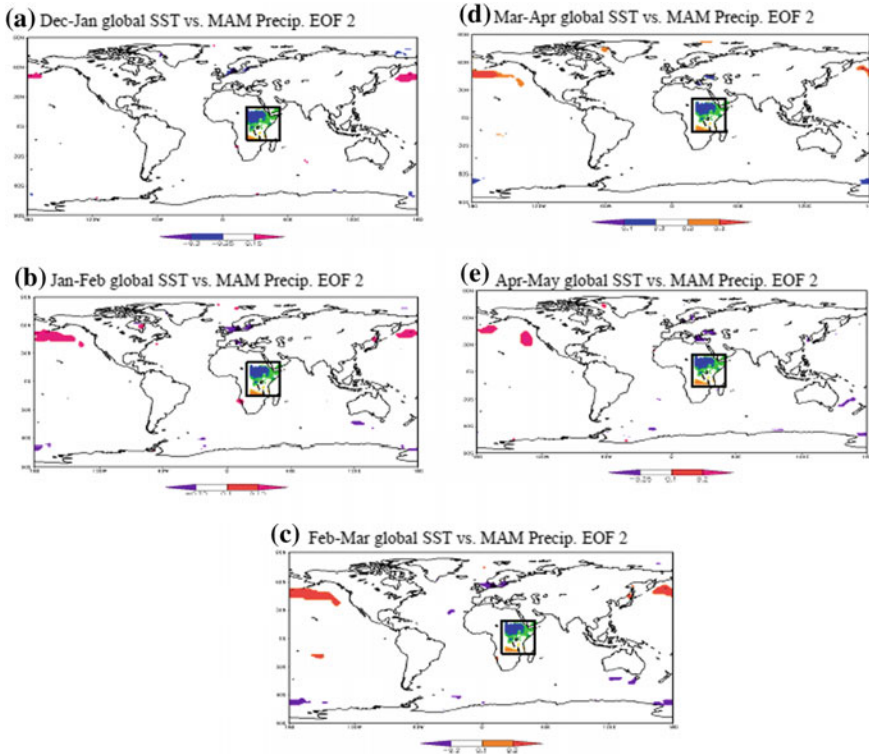
Fig. 3 Relationship between standardized bimonthly global SST anomalies and East African MAM precipitation EOF 2 time series at different time lags. Legend is for the range of correlation coefficient. Significant areas at 95% confidence level, using t-test, are *shaded*. The precipitation spatial patterns over the region are enclosed in *boxes*

persistent mid-latitude North Atlantic conditions (Fig. 4), which could be reminiscent of the Atlantic Multidecadal Oscillation (AMO). In contrast, the Pacific generally displayed an indirect relationship with the strongest (weakest) events captured in DJ (JF). No feature of climatological significance was observed over the Indian Ocean except a small-scale signal in AM, which resided in one of the arms of the IOD domain. Direct relationship between precipitation EOF 4 and the global SST was found to be impressively dominated by the Pacific (Fig. 5), peaking from MA to AM. The evolution of the Gulf of Guinea SST showed a progressive but abysmal development from DJ to MA, and thereafter decayed till the end of the rainy season. In tandem with this event was the detection of a North Atlantic SST pattern, also reminiscent of a small-scale AMO which persisted till the end of the study. The Indian Ocean's link to the precipitation mode was discernible from FM to AM.
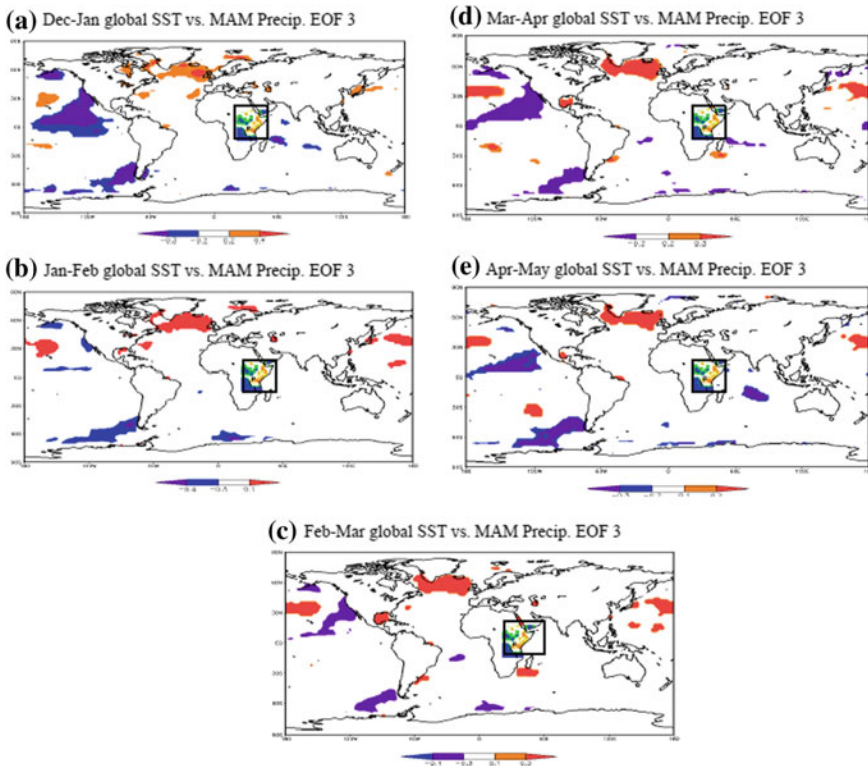
Fig. 4 Relationship between standardized bimonthly global SST anomalies and East African MAM precipitation EOF 3 time series at different time lags. Legend is for the range of correlation coefficient. Significant areas at 95% confidence level, using t-test, are *shaded*. The precipitation spatial patterns over the region are enclosed in *boxes*

3.3 Composites of Standardized Global-Scale Divergent Circulation Anomalies and East African MAM Precipitation Modes

On climate timescale, the boundary forcing emanating from, for example, the ocean surface drives atmospheric circulation. Since MAM precipitation EOF 2 seemed not to be well related to the global SST (Fig. 3), its atmospheric circulation would be excluded from this paper until this unusual observation is clarified through further studies possibly through numerical modeling. It is therefore instructive to focus on EOFs 1, 3, and 4, which is presented shortly.

Figures 6, 7 and 8 show the standardized global-scale velocity potential and divergent circulation anomalies at the upper atmosphere (200 hPa) in relationship to the MAM rainfall modes.
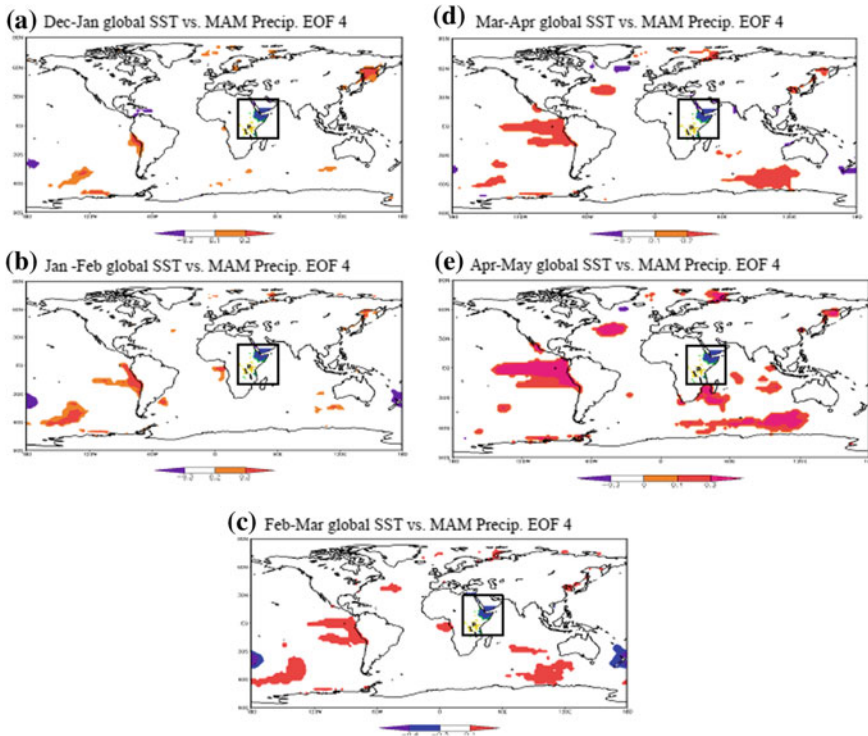
Fig. 5 Relationship between standardized bimonthly global SST anomalies and East African MAM precipitation EOF 4 time series at different time lags. Legend is for the range of correlation coefficient. Significant areas at 95% confidence level, using t-test, are *shaded*. The precipitation spatial patterns over the region are enclosed in *boxes*

With respect to MAM precipitation EOF 1, it was observed that upper level divergence was centered over the equatorial western Pacific from DJ to AM, but became weaker from MA to AM. Correspondingly, upper level divergence was located over Asia spreading to the Indian Ocean in DJ. In JF, there was a shift of the field more eastward over Asia, where it became more intensified. In tandem with this development was the formation of a smaller divergence center specifically located over the Indian Ocean. This signified convective development leading to rainfall over the ocean. However, a weak upper level convergence was found over GHA which suggested transport of weak subsidence anomalies of dry air mass from the upper atmosphere to the surface. This was indicative of a small rainfall deficit. In FM, the divergence center over Asia weakened, but the systems over the Indian Ocean and GHA persisted. In MA, an upper level divergence center, suggestive of Tropical East Jet (TEJ), was found over northern Africa. This co-occurred with a strong divergence center over the Indian Ocean. It appeared that the two centers were associated with a shift of the upper level convergence to the horn area, leading
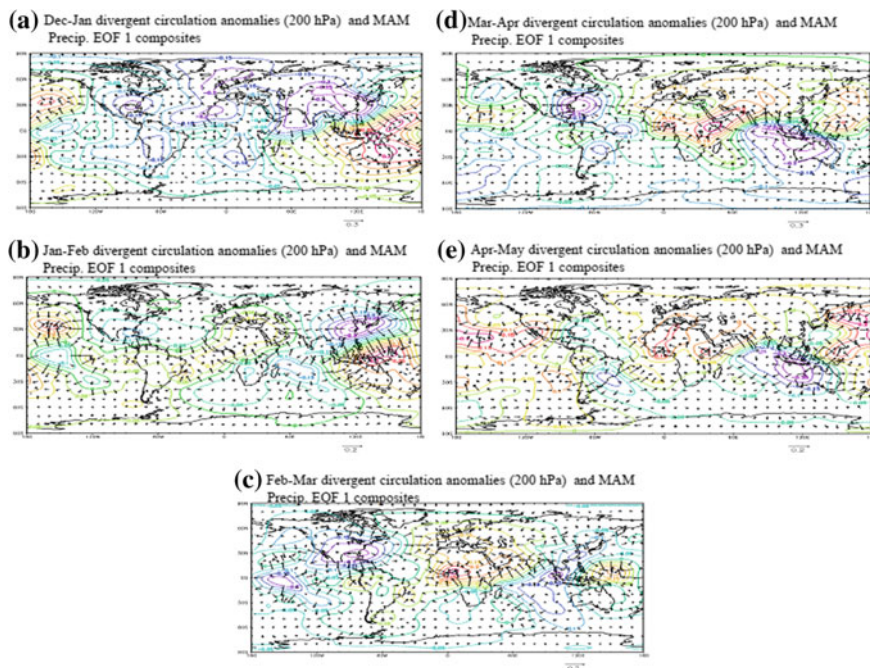
(a) Dec-Jan divergent circulation anomalies (200 hPa) and MAM Precip. EOF 1 composites

(d) Mar-Apr divergent circulation anomalies (200 hPa) and MAM Precip. EOF 1 composites

(b) Jan-Feb divergent circulation anomalies (200 hPa) and MAM Precip. EOF 1 composites

(e) Apr-May divergent circulation anomalies (200 hPa) and MAM Precip. EOF 1 composites

(c) Feb-Mar divergent circulation anomalies (200 hPa) and MAM Precip. EOF 1 composites

Fig. 6 Standardized bimonthly global divergent circulation anomalies and East African MAM precipitation EOF 1 mode composites at different time lags

to rainfall deficit. In AM, similar conditions persisted, but with disappearance of the TEJ-like feature.

In DJ and with respect to precipitation EOF 3, upper level divergence was located over equatorial western Pacific and over the GHA. There was a corresponding upper level convergence over the Indian Ocean (Fig. 7). Convective development leading to rainfall would occur over the region, in contrast to rainfall deficit over the Indian Ocean. Similar systems persisted from JF to MA, but the divergence center over the Pacific weakened. In AM, re-emergence of the divergent circulation was observed over the equatorial Pacific. While the upper level convergence over the Indian Ocean was maintained, the GHA divergence center disappeared. This was indicative of rainfall surplus (deficit) over the Pacific Ocean (GHA and Indian Ocean).

In DJ, the center of action of upper level convergence was located over equatorial western Pacific and Indian Oceans in relationship to precipitation EOF 4. No upper level divergence was detected over GHA, which was indicative of rainfall deficit. In JF, upper level divergence replaced convergence in the Pacific. This was accompanied by weak (strong) convergence over Indian Ocean (northern Africa), which persisted to FM. In MA, divergence developed over the equatorial central Pacific and the Indian Ocean, but a strong northern African convergence was
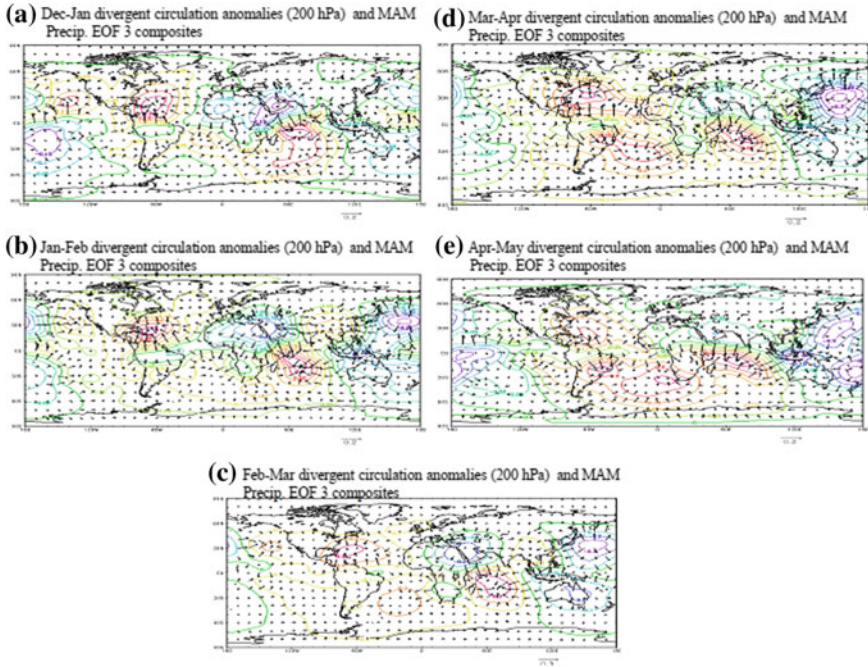
Fig. 7 Standardized bimonthly global divergent circulation anomalies and East African MAM precipitation EOF 3 mode composites at different time lags

observed. Finally, in AM the following observations were made: divergence over the central Pacific, convergent-divergent dipole system over the Indian Ocean, and disappearance of the northern African convergence.

4 Discussion

4.1 Standardized Global-Scale SST Anomalies and Their Associated Upper Level Divergent Circulation in Relationship to MAM Rainfall Modes

The boundary conditions of the ocean surface among other factors drive atmospheric circulations, including rainfall patterns, beyond weather timescale. In the study, four dominant MAM seasonal rainfall modes have identified. The spatio-temporal features were distinct but similar to earlier studies (e.g. Smith and Semazzi 2014). Several factors are known to contribute to MAM rainfall variability. Indeje et al. (2000) reported that local factors over the region played an important role. In a spatially remote sense, ENSO has been found to be the prime driver of the
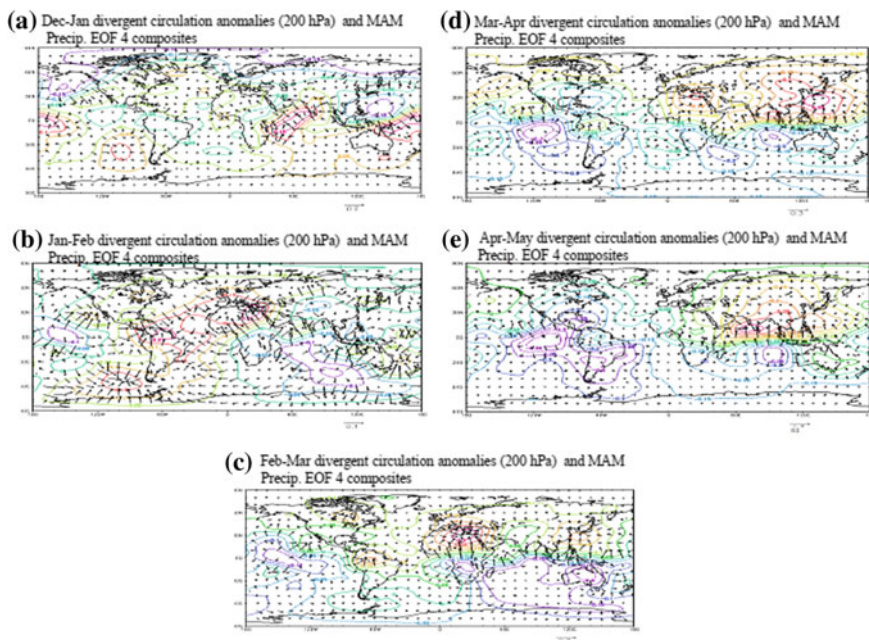
Fig. 8 Standardized bimonthly global divergent circulation anomalies and East African MAM precipitation EOF 4 mode composites at different time lags

interannual variability of the region's rainfall (Nicholson and Entekhapi 1986; Ogallo 1989).

In this study, even though the precipitation temporal patterns display low interannual variance (Ogallo 1989), their relationships with global SST distributions were distinct. In general, the modes responded differently to the Pacific, Atlantic, and Indian Oceans. They also differed with respect to specific oceanic sectors that corresponded to them. In particular, specific Niño regions were identified for each of the three precipitation modes as global ocean climate evolved with time. This underscored the importance of the Pacific, Atlantic, and Indian Ocean SST delineation for every timescale. In fact, the use of the bimonthly climate features has introduced a new picture in the oceanic conditions and their associated atmospheric structures modulating the rainfall variability. Comparison of this study with monthly and seasonal-scale features already studied over the same period (not shown) also supported the rationale of recognizing the important role of the bimonthly climate features in the East African climate system.

This study has revealed that over the Pacific key bimonthly warm (cold) oceanic features that drove or were in association with, the rainfall EOF 1 mode, representing El Niño (La Niña) tended to enhance (suppress) rainfall in GHA. The mechanism, however, was indirect and involved tropical Walker and Hadley

circulations. The role of the tropical Atlantic, as with the Pacific, was also critical. It was observed that a warming (cooling) of the tropical Atlantic enhanced (suppressed) convective development over the region. This was pronounced when the Atlantic started warming up in the Northern Hemisphere (NH) spring. The Indian Ocean also played a role to some extent which had similar effects or associations as with the other two oceans.

The poor relatedness between rainfall EOF 2 and global SST distributions needed further attention. In fact, Smith and Semazzi (2014) made a similar observation in their study. This observation warranted verification using other high resolution datasets or numerical modeling studies. The results from Fig. 4 indicated a persistent and a direct AMO-like relationship with precipitation EOF 3. This oceanic mode is an essential part of the Atlantic Meridional Overturning Circulation, which has a great influence on the region's climate. Positive (negative) AMO phase was linked to anomalous wetness (dryness) of GHA, which was consistent with literature. However, the spatial extent of the effects of or associations with, the AMO were not expected to be homogeneous. In contrast, the Pacific as a whole indicated an inverse relationship with the rainfall mode, but the strongest (weakest) events detected in DJ (JF) emphasized the climatological significance of ENSO in NH winter. The competition between AMO-like feature and ENSO was important in further understanding of the region's climate variability. A localized climatic signal detected in AM over southwestern Indian Ocean was indicative of the association of the region's climate with IOD (Saji et al. 1999; Marchant et al. 2006). While ENSO is known to be prominent in NH winter, the direct relationship between precipitation EOF 4 and the Pacific SST (Fig. 5) rather peaked from MA to AM. This suggested that the Niño regions have their specific decay times. The AMO-like feature captured in the North Atlantic had similar role as the one detected for EOF 3.

The standardized divergent circulation anomalies associated with the time-evolving global SST distributions and with respect to the three rainfall modes have been investigated. The importance of global divergent circulations in monsoon dynamics has been reported (Trenberth et al. 2000). In this study, composite analysis revealed that divergence (convergence) and the centers of action at 200 hPa level provided useful information on how the bimonthly atmospheric flows could be applied to explain the precipitation patterns. The distinction of the circulation patterns (Figs. 6, 7 and 8) were based on their strengths, locations, and spatial extents. Diabatic heating is known to provide energy for driving such circulation patterns in the global tropics (Trenberth et al. 2000).

In the proximity of GHA, upper level divergence would lead to cloud formation and consequently precipitation, depending on other factors. Upper level convergence would be associated with transport of dry air mass from the upper atmosphere to the surface, which would indicate drought conditions.

4.2   Implications for Climate Change Adaptations

From this study, the region may be viewed as vulnerable to climate extremes based on the spatio-temporal patterns of the rainfall variability. The specific oceanic features identified could be used in improving the region's seasonal climate prediction. Where the patterns consistently showed extreme dry or wet conditions, it calls for policy-driven adaptation agenda to contain the excesses of climate change. These should be directed to climate-sensitive socio-economic problems such as food insecurity, flood/drought and associated disasters, loss of biodiversity, and climate-driven human diseases. The overall goal could be achievable if end users are prompted of the need to incorporate the outcomes of this study into the existing information required for adaptation strategies.

5   Conclusion and Recommendations

The study primarily focused on analysis of bimonthly global-scale climate features and their relationship to the dominant MAM rainfall modes over the GHA during the climatologically prominent phase of ENSO. EOF analysis isolated four dominant modes, which together contributed to 34.2% of the total explained variance. Showing distinct spatio-temporal patterns, their time series were all characterized by interannual variability. Each of the modes responded differently to the five consecutive two months standardized oceanic anomalies from DJ to AM. Specific oceanic features were noted as having an influence on or having an association with, the rainfall modes. The Pacific Niño regions were the prime factors, though the Atlantic and the Indian Oceans had their share. The associated divergent circulation displayed varied patterns in terms of their action centers, spatial extents and intensities, and these were specific to precipitation EOFs 1, 3, and 4 modes. These gave further guidance in understanding convective development or otherwise over the region.

Traditionally, statistical models rely on seasonal climate features for predicting seasonal rainfall patterns. On the basis of this study, it would be useful if the specific bimonthly predictors were incorporated into the prediction scheme, to enhance climate change adaptations specific to a climatic setting. Rainfall EOF 2 practically did not relate well with the global SST, a situation which required further research. This was substantiated with monthly and seasonal SST analyses over the same period of study. Furthermore, this observation was in consonance with an earlier study. It became clear from this study that the EOF 2 mode was perhaps governed by complex system involving land-ocean-atmosphere feedbacks, which warranted modeling studies. Alternatively, the authors have begun to explore the EOF 2 issue using different datasets. Finally, the current study is being extended by the authors to the short rains.

References

Akponikpè, P. B., Ge´rard, I. B., Michels, K., & Bielders. C. L. (2010) Use of the APSIM model in long term simulation to support decision making regarding nitrogen management for pearl millet in the Sahel. *In Journal of European Agronomy, 32,* 144–154.

Barnston, A. G., & Ropelewski, C. F. (1992). Prediction of ENSO episodes using canonical correlation analysis. *In Journal of Climate, 17,* 1316–1345.

Bowden, J. H., & Semazzi, F. H. M. (2007). Empirical analysis of intraseasonal climate variability over the greater Horn of Africa. *In Journal of Climate, 20,* 5715–5731.

Ford, J. D., Berrang-Ford, L., Bunce, A., McKay, C., Irwin, M., & Pearce, T. (2015). The status of climate change adaptation in Africa and Asia. *In Regional Environmental Change, 15,* 801–814. doi:10.1007/s10113-014-0648-2

Funk, C. (2012). Exceptional warming in the Western Pacific-Indian Ocean Warm Pool has contributed to more frequent droughts in Eastern Africa. *In Bulletin of American Meteorological Society, 7,* 1049–1051.

Hannachi, A., Jolliffe, I. T., & Stephenson, D. B. (2007). Empirical orthogonal functions and related techniques in atmospheric science: A review. *In International Journal Climatology, 27,* 1119–1152. doi:10.1002/joc.1499

Harris, I., Jones, P. D., Osborna, T. J., & Lister, D. H. (2014). Updated high-resolution grids of monthly climatic observations—The CRU TS3.10 Dataset. *In International Journal of Climatology, 34,* 623–642. doi:10.1002/joc.3711

Indeje, M., Semazzi, F. H. M., & Ogallo, L. J. (2000). ENSO signals in East African rainfall seasons. *In International Journal of Climatology, 20,* 19–46.

Johnson, R. A., & Wichern, D. W. (2007). *Applied multivariate statistical analysis* (6th ed.). New Jersey, USA: Pearson Education, INC.

Kalnay, E., Kanamitsu, M., Kistler, R., Collins, W., Deaven, D., Gandin, L., et al. (1996). The NCEP/NCAR 40-year reanalysis project. *In Bulletin of American Meteorological Society, 77,* 437–471.

Krishnamurti, T. N. (1971). Tropical east-west circulations during the northern summer. *In Journal of Atmospheric Sciences, 28,* 1342–1347.

Latif, M., Dommenget, D., Dima, M., & Grotzner, A. (1999). The role of Indian Ocean sea surface temperature in forcing East African rainfall anomalies during December–January 1997/98. *In Journal of Climate, 12,* 3497–3504.

Marchant, R., Mumbi, C., Behera, S., & Yamagata, T. (2006). The Indian Ocean dipole—the unsung driver of climatic variability in East Africa. *In African Journal of Ecology*, *45*, 4–16.

Nicholson, S. E., & Entekhabi, D. (1986). The quasi-periodic behaviour of rainfall variability in Africa and its relationship to the Southern Oscillation. *In Archiv für Meteorologie, Geophysik und Bioklimatologie, 34,* 311–348.

North, G. R., Bell, T. L., Cahalan, R. F., & Moeng, F. J. (1982). Sampling errors in the estimation of empirical orthogonal functions. *In Monthly Weather Review, 110,* 699–706.

Ogallo, L. J. (1988). Relationships between seasonal rainfall in East Africa and the Southern Oscillation. *In International Journal of Climatology, 8,* 31–43.

Ogallo, L. J. (1989). The spatial and temporal patterns of the East African seasonal rainfall derived from principal component analysis. *In International Journal Climatology, 9,* 145–167.

Ropelewski, C. F., & Halpert, M. S. (1987). Global and regional scale precipitation patterns associated with the El Niño Southern Oscillation. *In Monthly Weather Review, 115,* 1606–1626.

Saji, N. H., Goswami, B. N., Vinayachandran, P. N., & Yamagata, T. (1999). A dipole mode in the tropical Indian Ocean. *In Nature, 401,* 360–363.

Schreck, C. J., & Semazzi, F. H. M. (2004). Variability of the recent climate of eastern Africa. *In International Journal of Climatology, 24,* 681–701.

Smith, T. M., & Reynolds, R. W. (2004). Improved extended reconstruction of SST (1854–1997). *In Journal of Climate, 17,* 2466–2477.

Smith, K. A., & Semazzi, F. H. M. (2014). The role of the dominant modes of precipitation variability over Eastern Africa in modulating the hydrology of lake victoria. *In Advances in Meteorology*, 11. Article ID 516762, http://dx.doi.org/10.1155/2014/516762

Tetteh, I. K. (2012). *West African seasonal climate variability and predictability*, PhD thesis, North Carolina State University.

Trenberth, K. E., Stepaniak, D. P., & Carbon, J. M. (2000). The global monsoon as seen through the divergent atmospheric circulation. *In Journal of Climate, 13,* 3969–3993.

Washington, R., Harrison, M., Conway, D., Black, E., Challinor, A., Grimes, D., et al. (2006). African climate change—Taking the shorter route. *In Bulletin of American Meteorological Society*, 1355–1366.

Wilks, D. S. (2006). *Statistical methods in the atmospheric sciences* (3rd ed.). New York, USA: Academic Press.